



Explosion of Liquid Metal Jets in the Cathode Spot of a Vacuum Arc

I.V. UIMANOV and G.A. MESYATS***

** Institute of Electrophysics UB RAS, Ekaterinburg, Russia*

106 Amundsen St., Ekaterinburg, 620016, Russia

e-mail: uimanov@iep.uran.ru

***Lebedev Physical Institute, Russian Academy of Sciences*

A **two-dimensional axisymmetric model** has been developed to describe the formation of a liquid metal jet, the droplet pinch-off and **temperature runaway** in the **droplet-jet neck** during melt splashing from the cathode crater in a vacuum arc. The development of hydrodynamic and thermal instabilities has been self-consistently simulated in a copper current-carrying liquid metal jet in the “inertial” mode of the melt splashing. In this case, a jet with a longitudinal velocity gradient is formed and the droplet-jet neck becomes unstable due to the action of capillary forces (**Rayleigh–Plateau instability**). As a result, the neck radius decreases rapidly and the droplet splits off. In a current-carrying jet, this process is accompanied by a strong increase in the current density in the neck and its rapid heating due to the Joule effect to a critical temperature at certain values of current from the cathode spot plasma. It is shown that the heating process has the nature of a **temperature runaway** and, accordingly, can lead to its electric explosion. Assuming a constant current density on the jet surface, its minimum “explosion” value was calculated depending on the diameter, velocity and initial temperature of the jet. It is shown that for craters and jets of low-current arcs this density does not exceed **10^7 A/cm²** and, accordingly, can be provided by the ion current from the plasma of the cathode spot.

The **explosion of the liquid metal jets** is considered to be the basic mechanism of the birth of new cathode spot cells [1-4]. According to **ecton model**, the appearance of new cathode spot cells is due to the interaction of a liquid-metal jet with dense cathode spot plasma [2]. With this important part played by the liquid-metal phase in the self-sustaining of a vacuum discharge, for a long time, a quantitative description of the hydrodynamic processes responsible for the jets and droplets formation was so far confined to estimating or very simplified calculations. The study of thermal processes was also limited only by the static case without taking into account the liquid metal jet dynamics [3, 4]. The melt splashing process in the cathode spot at crater formation can be considered by convention to occur in three stages [5]. At the first stage, the formation of a crater, an axisymmetric liquid-metal rim is formed. Previously, we performed a simulation of the first stage using a **two-dimensional axisymmetric model** [6, 7]. The simulation results for the velocity and exit angle of a liquid-metal jet are in good agreement with experimental data on droplet emission. At the second stage, the rim disintegrates, due to the azimuthal instability developing by the **Rayleigh–Plateau mechanism**, into individual cylindrical jets that form a **“crown”**. The second stage was investigated by us analytically in the framework of a **linear instability theory** [8-10].

The formation of **quasi-one-dimensional cylindrical jets** and the jet disintegration into **droplets** will be attributed to the third stage. For the first time, a quantitative description of the hydrodynamic processes of the jets formation during the cathode crater formation based on the Navier–Stokes equations was carried out by us in [5, 11]. First we proposed a simplified **two-dimensional axisymmetric model** of the jet formation on a **flat melt surface** under the action of a ring-shaped external pressure [5]. A more convenient **“spherical pipette” model** was developed in [11]. Within the framework of this model, a jet dynamics and the droplet pinch-off has been numerically simulated. Based on the obtained results and experimental data on the explosion of metal wires, we obtained estimates of the current density on the droplet surface at which we can expect the droplet-jet neck heating to a critical temperature due to Joule effect. The presented model is a further development of the approach [11]. Here, the jet dynamics is modeled taking into account the heating of the droplet-jet neck. Thus, the proposed model in this work is a self-consistent description of hydrodynamic and thermal processes during the formation of a current-carrying liquid metal jet.

The main goal of the proposed model is a self-consistent description of the development of **hydrodynamic** and **thermal instabilities** in a liquid metal jet, which is formed when the melt is splashing from the cathode microcrater (see Fig.1).

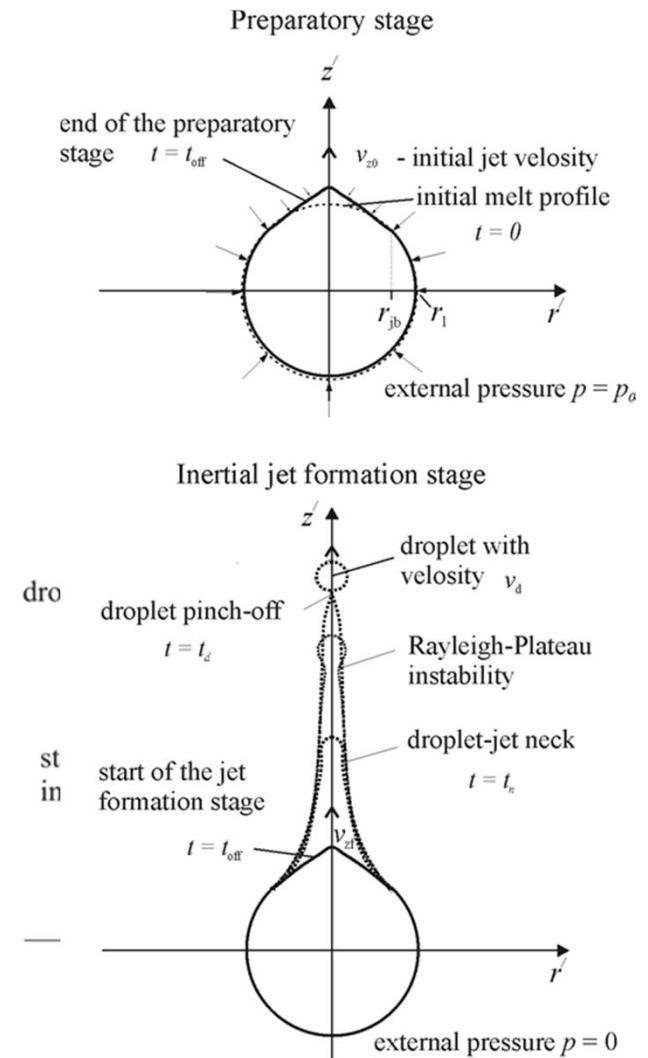
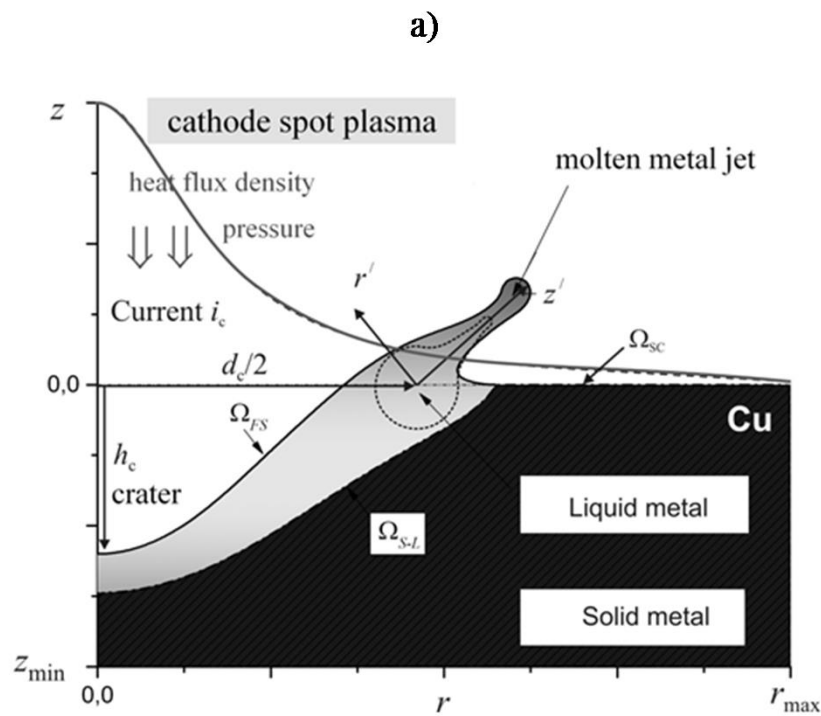


Fig. 1. Model geometry

$$j = -\sigma \nabla U_\Omega$$



Mathematical model

6

In this work, we will assume that the cathode spot plasma parameters change insignificantly on the scale of the jet submicrometer diameter. Then the current density that flows between the cathode spot plasma and the liquid metal jet j_S will be considered constant on the jet surface. To calculate the current density distribution in the jet $j = -\sigma \nabla U_\Omega$, the Laplace equation for the ohmic potential U_Ω is solved:

$$\frac{1}{r'} \frac{\partial}{\partial r'} \left(r' \sigma \frac{\partial U_\Omega}{\partial r'} \right) + \frac{\partial}{\partial z'} \left(\sigma \frac{\partial U_\Omega}{\partial z'} \right) = 0, \quad -\nabla U_\Omega \Big|_S = j_S / \sigma$$

$$\sigma \frac{\partial U_\Omega}{\partial r'} (r' = 0) = 0, \quad U_\Omega (z' = 0) = 0, \tag{1}$$

where σ is the electric conductivity of the melt. It is considered as a function of the jet temperature.

The jet temperature field $T(r', z', t)$ is calculated using the heat equation taking into account convective heat transfer:

$$c\rho \left(\frac{\partial T}{\partial t} + \vec{V} \nabla T \right) = \frac{1}{r'} \frac{\partial}{\partial r'} \left(r' \lambda \frac{\partial T}{\partial r'} \right) + \frac{\partial}{\partial z'} \left(\lambda \frac{\partial T}{\partial z'} \right) + \frac{j^2}{\sigma} \quad (2)$$

Here, t is time, c is the specific thermal capacity, λ is the thermal conductivity, ρ is the density, V is the hydrodynamic velocity of the melt in the jet, u , v are the radial and the axial velocity, respectively.

In general, the hydrodynamic part of the modeling scenario is similar to the “spherical pipette” model [11]. As sketched in the Fig. 1 the entire modeling process can be divided into two stages: preparatory and main (stage of the inertial jet formation, the droplet pinch-off and the development of the temperature runaway in the droplet-jet neck).

The top drawing in **Fig. 1** illustrates the **preparatory stage** of the simulation. At this stage $t < t_{\text{off}}$, the melt begins to move under the influence of external pressure p :

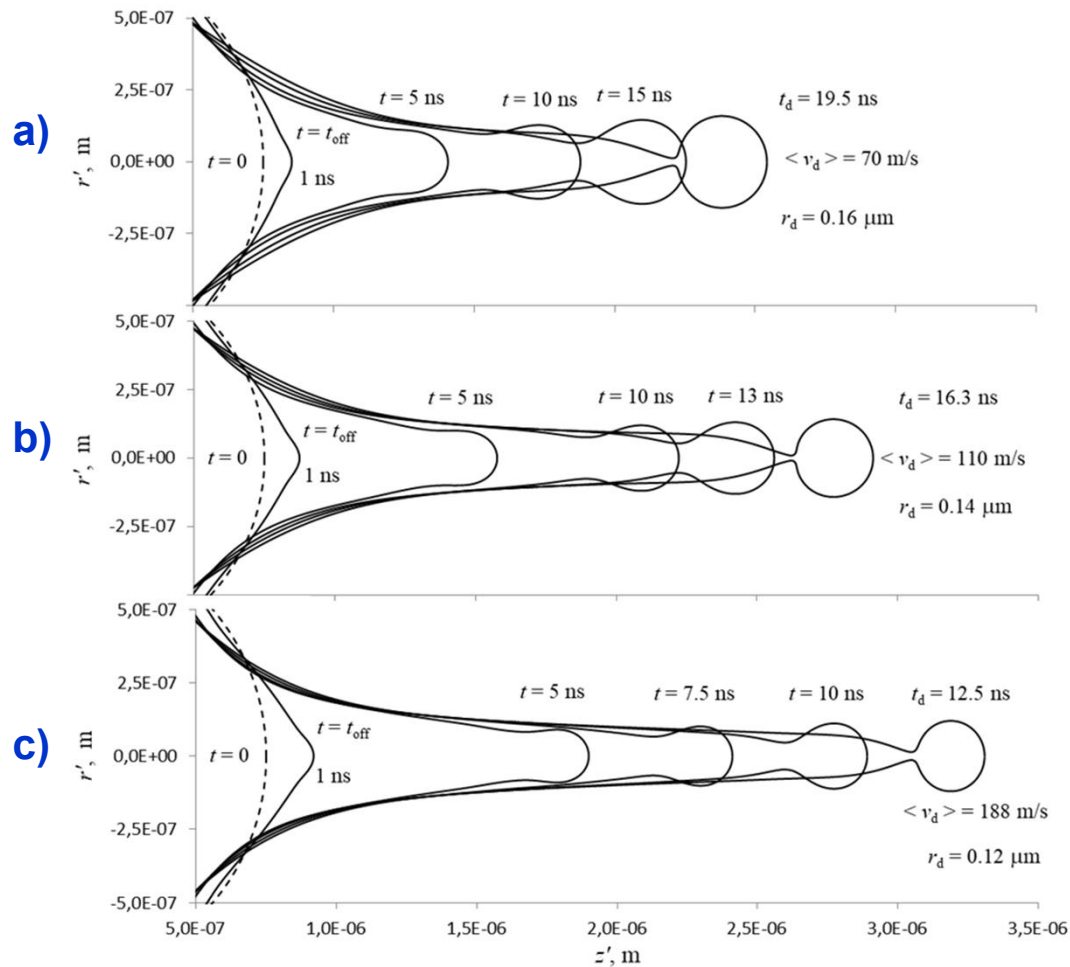
$$p = \begin{cases} p_0 f_p(t, t_{\text{off}}), & z' < 0 \quad \text{and} \quad z' > 0, \quad r' > r_{\text{jb}} \\ p_0 \exp\left\{-\left(\frac{l - r_{\text{jb}}}{r_{\text{jb}}}\right)^2\right\} f_p(t, t_{\text{off}}), & z' > 0, \quad r' > r_{\text{jb}} \end{cases} \quad (3)$$

where p_0 is the external pressure amplitude, $f_p(t, t_{\text{off}})$ (equal to 1 for $t < t_{\text{off}}$ and to 0 for $t > t_{\text{off}}$) is the Heaviside function that simulates the finite time of the pressure action during the formation of the jet, and l is the length of the envelope of the free surface, which is counted from $\{r_{\text{jb}}, z_p(t, r_{\text{jb}})\}$.

According (3) p is constant and equal to p_0 on most of the initial spherical surface of the melt. At the same time, it exponentially decreases to zero near the z' axis, creating “the pipette nozzle”. Varying the spatial parameters r_{jb} in (3), we can customize the jet diameter d_j . The initial velocity of the jet head, d_j , can be specified by properly adjusting p_0 and t_{off} . The top right drawing in **Fig. 1** illustrates the **preparatory stage** of the simulation.

At the main stage of modeling $t > t_{\text{off}}$, jet formation is calculated only under the action of inertia and surface tension forces. At the same time, the current density and temperature distribution in the jet is calculated self-consistently. As shown in bottom right picture of the **Fig. 1**, the jet elongation is accompanied by the formation of a droplet-jet neck at $t = t_n$. From this moment, a droplet begins to form on the jet head. Further, the neck radius r_n rapidly decreases, and the radius of the forming droplet r_d slightly increases. This leads to a significant increase in the current density and the Joule heat power in the **droplet-jet neck**. At time $t = t_d$, the neck breaks and the droplet pinch-off from the jet.

Thus, the external parameters of the problem are p_0 , r_l , r_{jb} , t_{off} , T_0 and j_S . As the main calculated parameters of the jet dynamics, we will use t_n , t_d , $\langle v_d \rangle$ and r_d , where $\langle v_d \rangle$ is the droplet average velocity along the $z/$ axis after pinch-off, r_d is the droplet radius. The main calculation parameter of the thermal part of the problem is the smallest surface current density j_{exp} at which there is a **temperature runaway** in the **droplet-jet neck**.



Calculated parameters:

$$r_{jb} = 0.5 \mu\text{m}, r_1 = 1.5 r_{jb}, t_{off} = 1 \text{ ns}, T_j = 2000 \text{ K}$$

Calculations were carried out for a copper cathode in the melt temperature range of 2000 - 5000 K. By choosing the external parameters of the problem, we simulated the dynamics of jets with a diameter of $d_j \sim 0.3 \mu\text{m}$ and an initial velocity $v_{z0} \sim 200 - 300$ m/s.

Fig. 2. The dynamics of the jet cross-sectional profile before droplet pinch-off in case of the temperature runaway in the droplet-jet neck for various initial jet velocities and the surface current densities j_{exp} : formation and droplet pinch-off in the inertial melt splashing mode at various pressures:

- a) $v_{z0} = 208$ m/s, $j_{exp} = 5 \cdot 10^6$ A/cm²,
- b) $v_{z0} = 250$ m/s, $j_{exp} = 6.5 \cdot 10^6$ A/cm²,
- c) $v_{z0} = 293$ m/s, $j_{exp} = 7.6 \cdot 10^6$ A/cm²

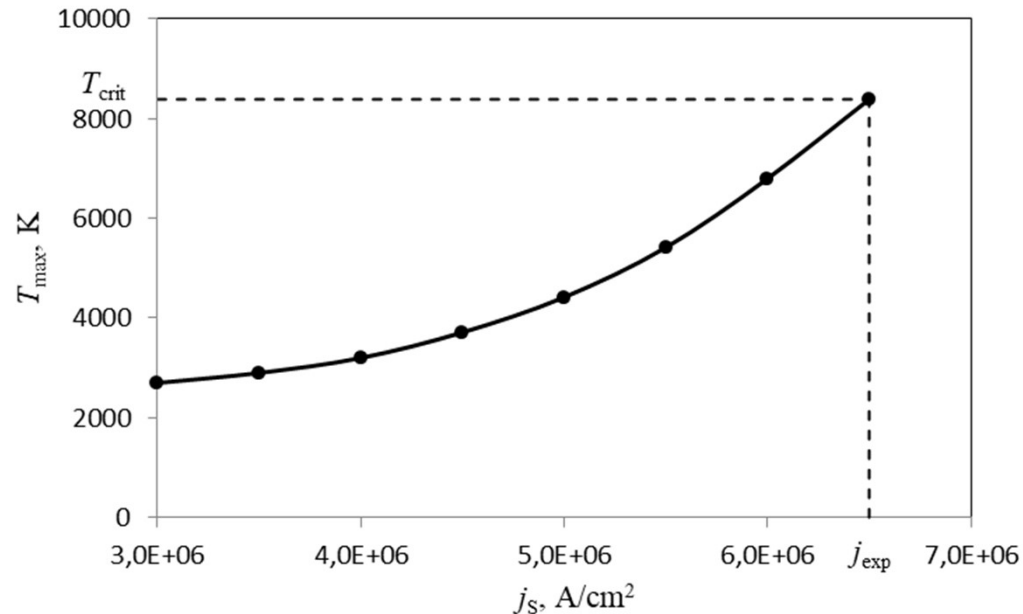
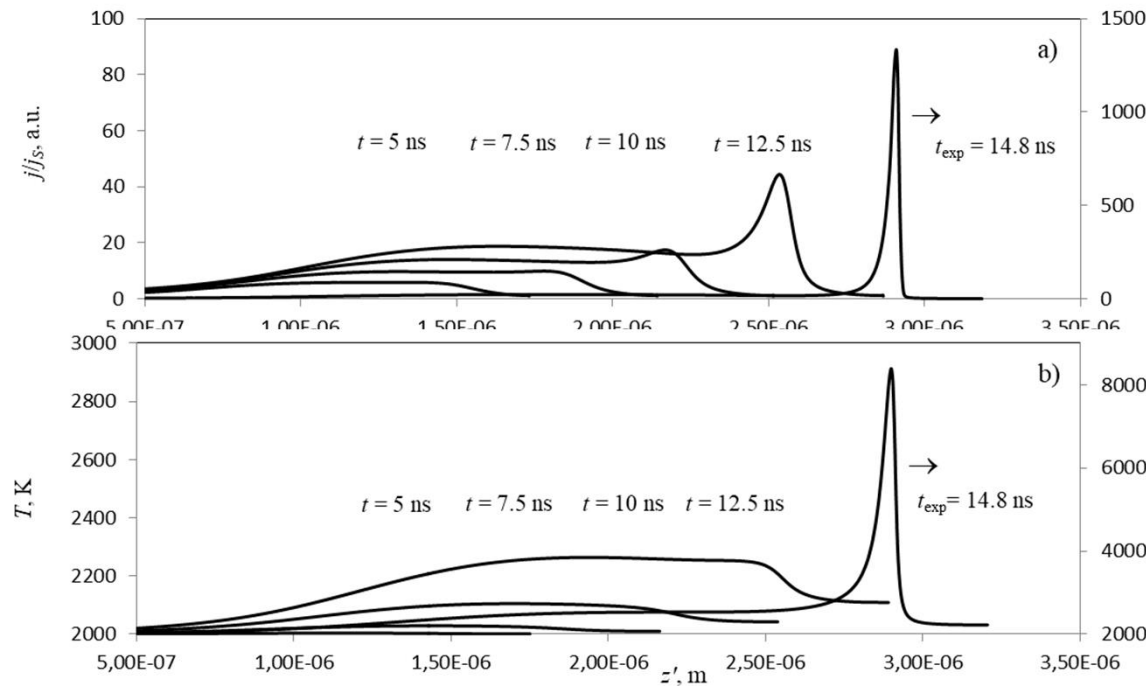


Fig. 3. Maximum jet temperature as a function of surface current density. The dynamics of the jet cross-sectional profile for $j_S = j_{exp} = 6.5 \cdot 10^6$ A/cm² is shown in the Fig. 2 b).

Calculated parameters: $r_{jb} = 0.5 \mu\text{m}$, $r_1 = 1.5 r_{jb}$, $t_{off} = 1\text{ns}$, $T_0 = 2000$ K, $v_{z0} = 250$ m/s.

Figure 3 shows the dependence of the maximum temperature in the jet on the jet surface current density j_S . According to the presented results, there is a **“explosion” surface current density j_{exp}** at which the droplet-jet neck is heated to a critical temperature.

In the cases $j_S < j_{exp}$, the **hydrodynamic instability** develops faster than the **thermal instability**.



Temporal evolution of the current density and temperature distributions along the jet is presented in Fig. 4 a) and b), respectively. Here, these distributions are shown on the right axis at $t = t_d$ ($t_{\text{exp}} \sim t_d$).

The time dependence of the radii of the droplet-jet neck r_n is presented in the Fig. 5.

Fig. 4. Temporal evolution of the current density a) and temperature b) distributions along the jet (along the z' axis at $r' = 0$). The dynamics of the jet cross-sectional profile is shown in the Fig. 2 b). Calculated parameters: $r_{\text{jb}} = 0.5 \mu\text{m}$, $r_1 = 1.5 r_{\text{jb}}$, $t_{\text{off}} = 1\text{ns}$, $T_0 = 2000$ K, $v_{z0} = 250$ m/s.

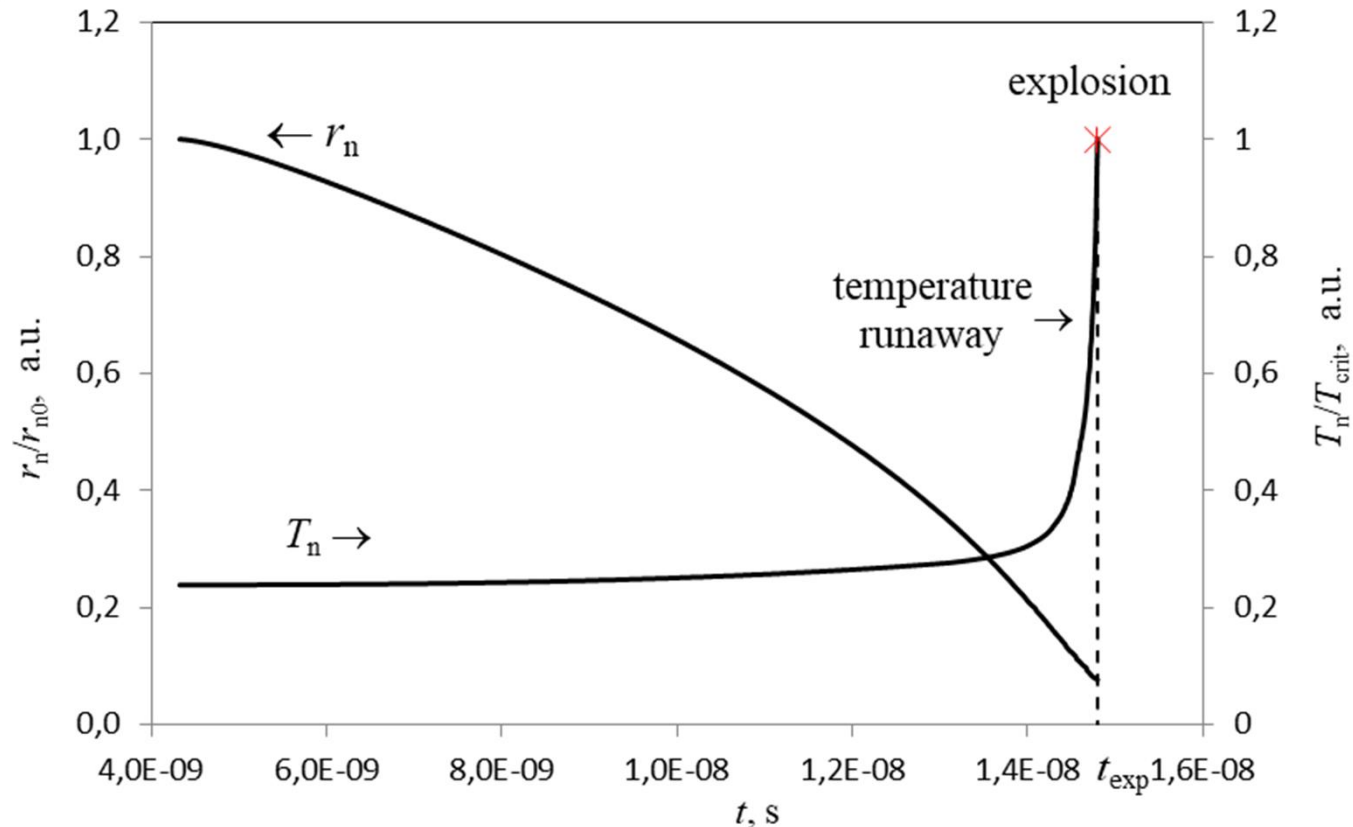


Fig. 5. The droplet-jet neck radius and maximum temperature versus time (the self-consistent modeling of **hydrodynamic** and **thermal instabilities**). The dynamics of the jet cross-sectional profile is shown in the **Fig. 2 b**).

Calculated parameters: $r_{jb} = 0.5 \mu\text{m}$, $r_1 = 1.5 r_{jb}$, $t_{\text{off}} = 1\text{ns}$, $T_0 = 2000 \text{K}$, $v_{z0} = 250 \text{m/s}$.

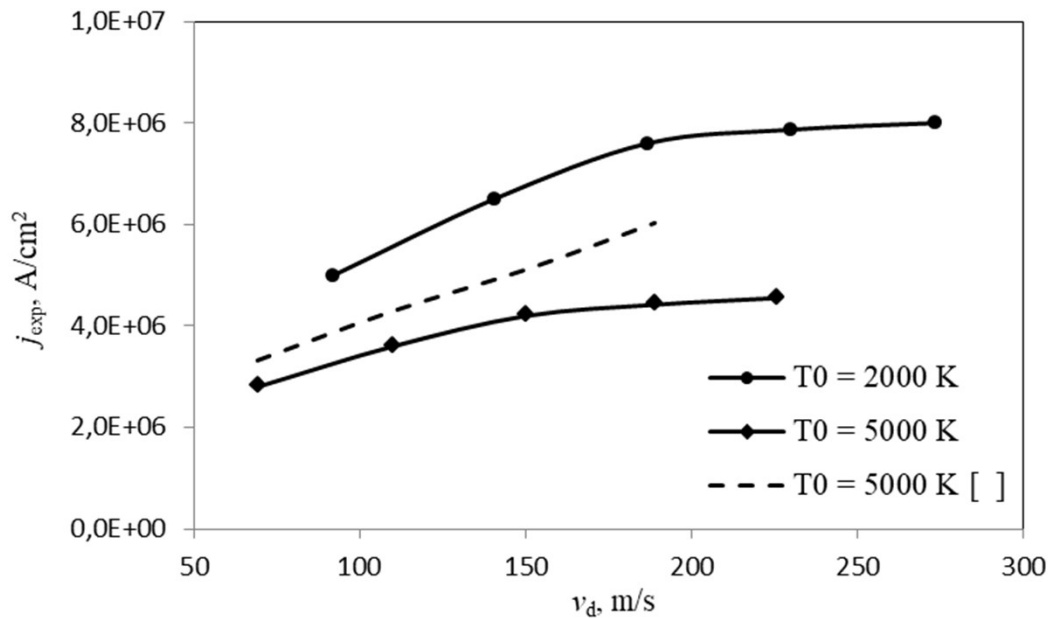


Fig. 6. The explosion surface current density j_{exp} as a function of the droplet velocity at different initial jet temperatures. The estimates we obtained in the framework of a not self-consistent approach [11] are shown by a dashed line for comparison.

As can be seen from the figure, the results of both approaches are in good agreement and the “explosion” surface current density does not exceed 10^7 A/cm² for all presented simulation cases. With an increase in the jet velocity, the rate of development of **hydrodynamic instability** (the rate of decrease in the neck radius) increases and, accordingly, the time of existence of the droplet-jet neck decreases. Therefore, a high j_{exp} is required to heat the neck to a critical temperature. However, in the case of a self-consistent approach, j_{exp} is somewhat lower and its dependence on the jet velocity (droplet velocity) tends to saturation (see Fig. 6).

Self-consistent modeling of the development of hydrodynamic and thermal instabilities in a current-carrying liquid metal jet formed during the splashing of metal from a cathode crater of the vacuum arc is carried out. The explosion surface current density from the cathode spot plasma j_{exp} , which is necessary for heating the droplet-jet neck to a critical temperature, is calculated. It does not exceed 10^7 A/cm² for droplets with a diameter of ~ 0.3 μm and a velocity of $200\div 300$ m/s and can be provided by the ion current from the cathode spot plasma [16]. It was shown that the droplet-jet neck heating with j_{exp} mainly occurs in the nonlinear stage of hydrodynamic instability due to the large coefficient of enhancement of the current density in the neck. Note that heating process of the collapsible droplet-jet neck has the nature of a temperature runaway. Therefore, the processes of droplet pinch-off and temperature runaway in a current-carrying liquid metal jet can provide the appearance of explosive plasma and thereby determine the **mechanism of the birth of new cells of the cathode spot of a vacuum arc.**

Acknowledgment

This work was supported in part by RFBR Grant Nos. 18-0800547, 19-08-00783, 19-58-53006.

1. G A Mesyats and D I Proskurovsky 1989 *Pulsed Electrical Discharge in Vacuum* (Berlin: Springer) pp 110–114.
2. G A Mesyats, *Cathode Phenomena in a Vacuum Discharge: The Breakdown, the Spark and the Arc* (Nauka, Moscow) pp 167–17, 2000.
3. G A Mesyats, JETP Lett., vol. 60, pp. 593–596, April 1994.
4. E A Litvinov, G A Mesyats, A G Parfenov and A I Fedosov, Zh. Tekh. Fiz., vol. 55, p. 2270, May 1985.
5. G A Mesyats and I V Uimanov, “Simulation of the Generation of Jets and Drops by the Cathode Spot of a Vacuum Arc,” in *Proc. of the 28th Inter. Symp. on Discharges and Electrical Insulation in Vacuum*, New York: IEEE, vol. 2, pp. 397–400, 2018.
6. G.A. Mesyats and I.V. Uimanov, IEEE Trans. on Plasma Sci., vol. 43, no. 8, pp. 2241–2246, Aug. 2015.
7. G.A. Mesyats and I.V. Uimanov, IEEE Trans. on Plasma Sci., vol. 45, no. 8. pp. 2087–2092, Aug. 2017.
8. M.A. Gashkov, N. M. Zubarev,, O. V. Zubareva, G. A. Mesyats and I. V. Uimanov, Journal of Experimental and Theoretical Physics, vol. 122, no. 4, pp. 776–786, 2016.
9. M.A. Gashkov, N.M. Zubarev, G.A. Mesyats, and I.V. Uimanov, Pis'ma Zh. Tekh. Fiz., vol. 42, no. 16, pp. 48–55, 2016.
10. M.A. Gashkov, G. A. Mesyats, N. M. Zubarev, I. V. Uimanov, IEEE Trans. Plasma Sci., vol. 47, no. 8, pp. 3456–3461, 2019.
11. I V Uimanov and G A Mesyats, *J. of Phys.: Conf. Ser.*, vol. 1393, p. 012034, 2019.
12. T J. Eggers, Phys. Rev. Lett., vol. 89, p. 084502–1, Aug. 2002.
13. M. Moseler and U. Landman, Science, vol. 289, pp. 1165–1169, Aug. 2000.
14. J. Eggers and E. Villermaux, “Physics of liquid jets,” Rep. Prog. Phys., vol. 71, p. 036601 (79pp), 2008.
15. X. D. Shi, M. P. Brenner and S. R. Nagel, Science, vol. 265, pp. 219-222, 1994.
16. I. V. Uimanov, IEEE Trans. on Plasma Sci., vol. 31, no. 5, pp. 822-826, 2003.